UDC 621.372.413

ELECTROMECHANICALLY TUNABLE DIELECTRIC MICROWAVE DEVICES

Yuriy V. Prokopenko, Yuriy M. Poplavko and Vitaliy I. Molchanov

National Technical University of Ukraine "KPI", Kyiv, Ukraine

High-tunable low-loss microwave dielectric devices are designed by electromechanical alteration in the configuration of device components. Specifically, this device consists of dielectric and metallic parts with an air gap between them. The gap location provides the largest perturbation in the electromagnetic field and a mini-actuator controls the device. Through experiments conducted, we test and apply the high-tunable dielectric resonators and filters as well as wide-band low-loss phase shifters.

Introduction

Application of high-tunable passive components, such as tunable resonators, phase shifters, is one of the current trends of modern telecommunication systems development. The components are key elements of smart antennas, phased-array antennas, tunable oscillators, filters and so on. The passive tunable components have to maintain low-loss and high quality factor. Only mechanical controlling system provides acceptable losses, especially in the millimeter wave range from various ways of implementing the tunable microwave system. Losses grow rapidly with the frequency increase for other tuning manners. Specifically, components are widely used in the decimeter and centimeter waves for tuning by the magnetic or electric fields. They are tuning of ferrite material permeability $\mu(H)$ by magnetic field, alteration of semiconductor material conductivity $\sigma(E)$ by electric field [1–3] or controlling of ferroelectric material permittivity $\varepsilon(E)$ by electric field [4–6]. Most of them have the frequency limitation of about 30–40 GHz. Optical tuning that exploits conductivity change $\sigma(\Phi)$ [7, 8] under light beam Φ also inserts considerable loss especially in the millimeter waves. Therefore, usual tunable components that use materials with controlled intrinsic properties of $\mu(H)$, $\sigma(E)$, or $\varepsilon(E)$ are characterized by essential insertion losses and have fundamental limitations in millimeter waves.

Hence, mechanical tuning is very promising to produce low insertion loss combined with good tunability in microwave subsystems. In other tuning techniques microwaves interact with the "active" material (ferrite, semiconductor, or ferroelectric) which is a part of microwave line, and the transmitted energy is partially absorbed by this material. On the contrary, mechanical system of control is not a part of microwave propagation route. So it does not contribute to the microwave loss. One crucial disadvantage of the mechanical control is a relatively slow tuning speed of microwave devices.

In 1984 the concept of piezoelectric actuators application for mechanical alteration was developed [9]. The concept was elaborated later for several microwave devices [10, 11]. Recent achievements in piezoelectric actuator and microelectromechanical system (MEMS) technologies take a big leap revealing new ways to combine advantages of mechanical and electrical tuning techniques. However, a tuning system should be highly sensitive to rather small displacement of device components for such applications.

The key idea of achieving such high sensitivity of system characteristics to small displacement of device parts is providing a strong perturbation of the electromagnetic field in the domain influenced directly by the mechanical control. To this end, a tunable dielectric discontinuity (the air gap) is created perpendicular to the pathway of the electric field lines. This air gap is placed between the dielectric parts or the dielectric plate and an electrode. An alteration of air gap dimension leads to the essential transformation of electromagnetic field and revising of such components characteristics as resonant frequency, phase of propagated wave and so on. This concept is illustrated for several microwave devices below.

Dielectric-air structure as a tunable component

Fig 1. presents the simplest structure suitable for electromechanical alteration of microwave characteristics. Two dielectrics are placed between infinite metal plates in this structure. The thickness d of the dielectric in the domain 2 may be variable.

Electromagnetic field of this structure may be described in terms of LM and LE modes [12]. A transverse wavenumber of the LM mode can be derived from dispersion equations:

$$\frac{\beta_{y1}}{\varepsilon_1}\tan(\beta_{y1}h)+\frac{\beta_{y2}}{\varepsilon_2}\tan(\beta_{y2}d)=0;$$
$$(\varepsilon_1-\varepsilon_2)k^2=\beta_{y1}^2-\beta_{y2}^2, \quad (1)$$

where β_{y1}, β_{y2} are the transverse wavenumbers in the domains 1 and 2, respectively; ε_1, ε_2 are the permittivities of dielectrics in the domains 1 and 2; h, d are the thicknesses of dielectrics in domains 1 and 2, $k=\omega/c$ is the wavenumber of free space; ω is the circular frequency; c is the light velocity in vacuum.

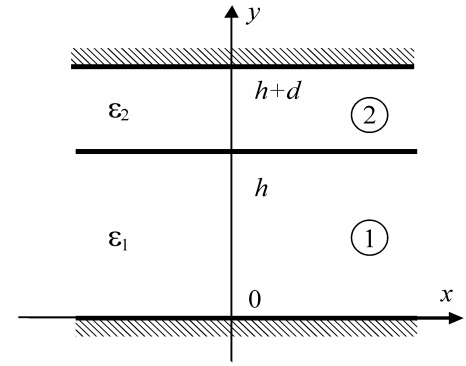

Fig. 1. One-dimensional dielectric discontinuity.

Using the equations (1) the calculations of the transverse wavenumbers are carried out in a wide range of the permittivities and thicknesses of dielectrics in domains 1 and 2. We discover that the transverse wavenumbers as the solutions of equations (1) depend on frequency, permittivities of dielectrics and sizes of domains 1 and 2. Fig. 2 shows the results obtained. Specifically, this figure illustrates a dependence of normalized transverse wavenumber of domain 1 versus the normalized air gap for frequencies presented by normalized wavenumber $kh=2$ and various permittivities of dielectric in the domain 1 while permittivity of the domain 2 is $\varepsilon_2=1$.

Transverse wavenumber of LM mode is very sensitive to variation of air gap between the dielectric and metal plate. The change in only tenth or even hundredth part of percent from size of dielectric in the domain 1 is sufficient for considerable alteration of transverse wavenumber. The required absolute change of air gap for significant alteration is not more than tens or hundreds micrometers depending on wavelength band and permittivity of the domain 1.

In contrast to LM mode distribution of electromagnetic filed of LE mode is significantly less sensitive to variation of air gap. Fig. 3 illustrates a dependence of transverse wavenumber β_{y1} of the fundamental LE mode on the normalized air gap thickness for various permittivities of the domain 1. For the LE mode required change of air gap is comparable with the size of dielectric in the domain 1 and quantitatively the alteration is appreciably less than for the LM mode.

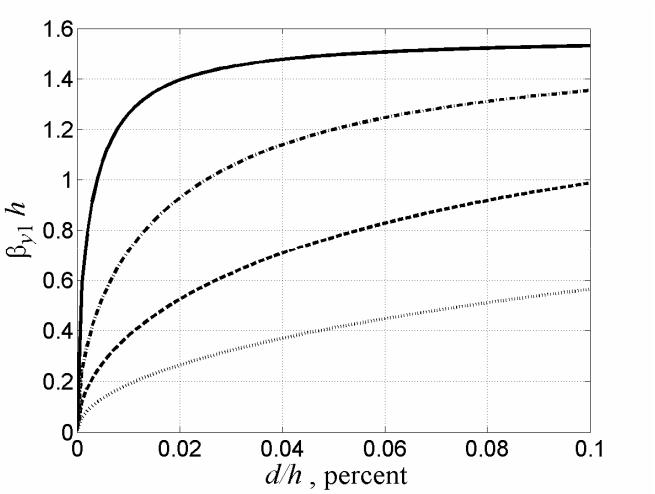

Fig. 2. Normalized transverse wavenumber of fundamental LM mode versus normalized air gap size for normalized wavenumber $kh=2$ and various permittivities of dielectric in the domain 1: $\varepsilon_1=10$ (dotted line); $\varepsilon_1=20$ (dash-dot line); $\varepsilon_1=40$ (dashed line); $\varepsilon_1=100$ (solid line).

The specificity of the LM mode is the existence of E_y-component of electrical field directed normally to the border of dielectric discontinuity. The component E_y is equal to zero for the LE mode. Therefore to achieve considerable alteration of electromagnetic field the border between dielectric and air should be located to perturb normal component of the electrical field. This principle is applied to all of microwave devices considered below.

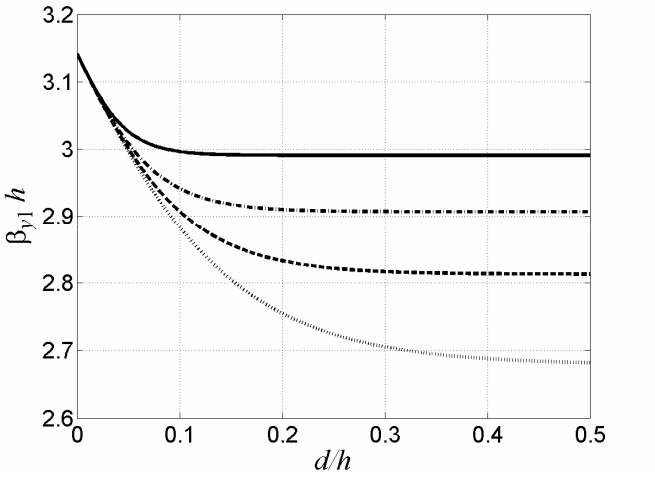

Fig. 3. Normalized transverse wavenumber of fundamental LE mode versus normalized air gap size for varied permittivities of dielectric in the domain 1: $\varepsilon_1=10$ (dotted line); $\varepsilon_1=20$ (dash-dot line); $\varepsilon_1=40$ (dashed line); $\varepsilon_1=100$ (solid line). Normalized wavenumber of free space is $kh=2$.

Tunable partially filled waveguide

The electrical field of a basic mode of the rectangular waveguide is directed parallel to a narrow wall of the waveguide. A border between dielectric and air should be located parallel to a wide wall of the waveguide (as shown in Fig. 4) to achieve a considerable perturbation of the electromagnetic field.

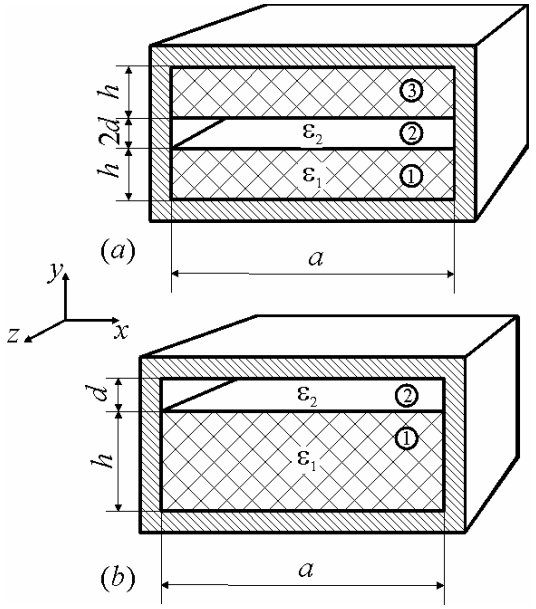

Fig. 4. Partially filled waveguide: (*a*) symmetrical design; (*b*) asymmetrical design.

The propagation constant of a basic mode of partially filled waveguide is given by the expression:

$$\beta_z = 2\pi / \lambda_w = \sqrt{\varepsilon_1 k^2 - (\pi / a)^2 - \beta_{y1}^2}\,, \qquad (2)$$

where a is the width of the waveguide; λ_w is the wavelength in the waveguide and β_{y1} is the solution of equations (1).

Fig. 5 illustrates the dependence of the normalized propagation constant augment on normalized air gap thickness for a waveguide with $h/a = 0.5$ at the frequency characterized by the normalized wavenumber $kh = 0.6$. The augment of normalized propagation constant has a simple meaning: it defines a phase shift of a waveguide section with a length equal to the thickness of dielectric. It should be remarked that the sensitivity of the phase shift to alteration of the air gap increases with a permittivity gain. At the same time a maximal phase shift is reduced when permittivity increases.

The last phenomenon can be easily explained through the equation (2) because the maximal increment of normalized transverse wavenumber $\beta_{y1}h$ is limited by the value of $\pi/2$. Hence, the selection of appropriate dielectric for phase shifter is a compromise between reducing the controlling voltage of an actuator and the waveguide section length.

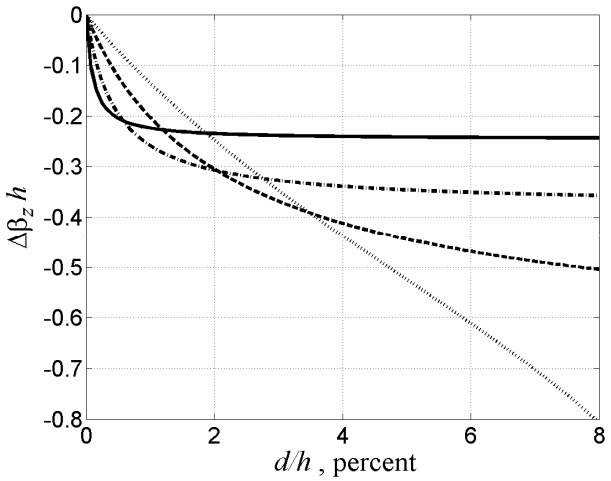

Fig. 5. The augment of normalized propagation constant versus normalized air gap size for certain permittivities of dielectric: $\varepsilon_1 = 10$ (dotted line); $\varepsilon_1 = 20$ (dash-dot line); $\varepsilon_1 = 40$ (dashed line); $\varepsilon_1 = 100$ (solid line). Normalized wavenumber of free space is $kh = 0.6$.

We suppose it is convenient to characterize wave propagation conditions by the effective permittivity of a partially loaded waveguide. It can be interpreted as a permittivity of a fully loaded waveguide which gives numerically the same propagation constant as partially loaded waveguide. For a basic mode of the rectangular waveguide the effective permittivity can be found as:

$$\varepsilon_{eff} = [(\pi / a)^2 + \beta_z^2] / k^2 = \varepsilon_1 - \beta_{y1}^2 / k^2\,.$$

Results of effective permittivity simulation are presented in Fig. 6. The air gap heavily influences effective parameters, especially for high-ε materials. The key reason for such high sensitivity is the location of dielectric discontinuity. The air gap is located across the electrical field of a waveguide basic mode and effects as strong perturbation of the electromagnetic field quantitatively dependent on the air gap size *d*. The fact is well known for the waveguide technique of dielectric permittivity measurement. The air gap between dielectric material and wide wall of waveguide dramatically reduces a measured value of dielectric permittivity. In addition, it is the main component of measurement uncertainty. However, the phenomenon is applicable for the development of tunable devices.

Dielectric constant is a critical parameter to determine a signal propagation constant. Therefore, one of the possible ways of utilizing effective permittivity transformation is developing phase shifters. Wavelength in dielectric filled part of waveguide is shortened

proportionally to $\varepsilon_{eff}^{1/2}$. Because of partial loading of waveguide, there is the nonzero component E_z of electric field in the propagation direction. In combination with the component E_y orthogonal to the media boundary it gives a resultant vector $\mathbf{E}$, crossing a media boundary at some slope. There is also a refraction caused by the difference in dielectric properties.

Thus a traveling wave makes a two-way path: one inside a dielectric and another one in the air. Refraction causes the ratio of the ways in the dielectric and air to change as the air gap varies. A phase shift of the traveling wave can be controlled by varying the part of the way that a wave takes outside the dielectric.

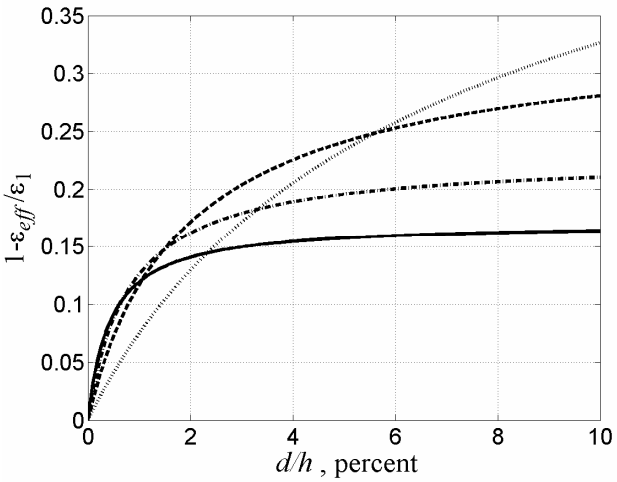

Fig. 6. Effective permittivity of a partially loaded waveguide for certain permittivities of the dielectric: $\varepsilon_1 = 10$ (dotted line); $\varepsilon_1 = 20$ (dash-dot line); $\varepsilon_1 = 40$ (dashed line); $\varepsilon_1 = 100$ (solid line).

This idea was experimentallly verified. The phase shifter was made inside a rectangular waveguide section. It can be made either in a symmetric or asymmetric fashion (the last one is shown in Fig. 7). A controlled element consists of a dielectric slab supported by the metal plate. This plate is rigidly attached to the piezoelectric actuator. Under applied control voltage the air gap size d is controlled through actuators' variable extension.

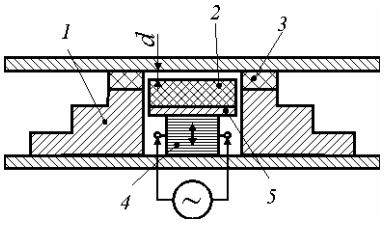

Fig. 7. Experimentally studied setup of the waveguide phase shifter: (*1*) matching section; (*2*) dielectric; (*3*) dielectric transformer; (*4*) actuator; (*5*) metallization.

Fig. 8 illustrates the measured control curves of the waveguide phase shifter for different dielectrics: Al_2O_3 ($\varepsilon = 11.6$, $\tan\delta = 0.7 \cdot 10^{-4}$); (Mg,Ca)$TiO_3$ ($\varepsilon = 21$, $\tan\delta = 2 \cdot 10^{-4}$); $BaTi_4O_9$ ($\varepsilon = 37$, $\tan\delta = 3 \cdot 10^{-4}$); BLT $\varepsilon = 85$, $\tan\delta = 2 \cdot 10^{-3}$). The control curves have almost linear character and promising values of a phase shift. Fig. 9 demonstrates the measured *S*-parameters of the phase shifter. The main component of insertion loss is a reflection of the incident wave due to mismatching of characteristic impedances of an active waveguide part with movable dielectric and input/output sections of the waveguide. This parameter could be improved by optimization of matching section. It is expected that increasing the operation frequency can make this design competitive with solid state devices.

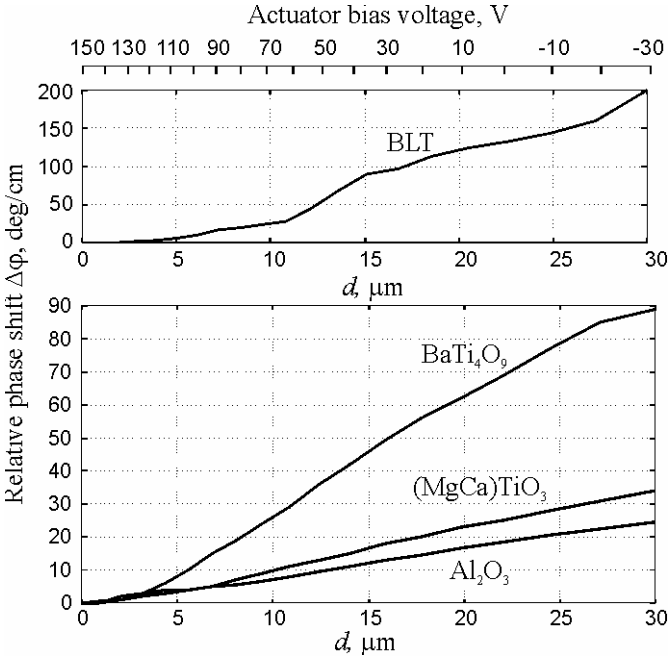

Fig. 8. Measured control curves for waveguide phase shifter at 10.5 GHz frequency.

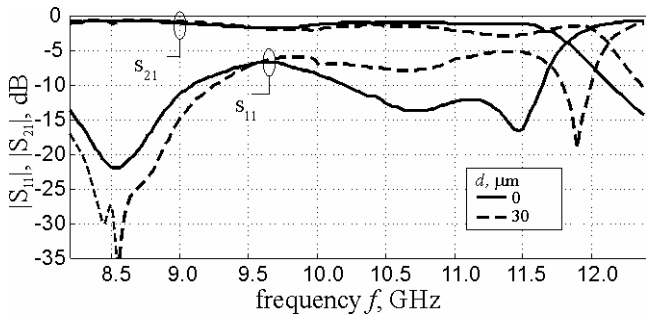

Fig. 9. Measured S-parameters of the waveguide phase shifter on the dielectric plate of 1mm height and 10 mm length with $\varepsilon_1 = 21$ permittivity.

Tunable dielectric resonators

The electromechanical manner of high-quality dielectric resonator (DR) frequency control is well known. One of the examples is two cylindrical DRs with the $TE_{01\delta}$ mode separated by the air slot, constituting a binary DR [13]. Lowest resonant frequency tuning of the binary DR reaches several percent while alteration of air slot is comparable with its sizes. The binary DR is not suitable for piezo-actuator or MEMS control because of such large displacement of its parts.

Electrical field components in the binary DR are located in its basis plane. In contrast to the binary DR a split dielectric resonator (SDR) [14], notably of $TE_{01\delta}$ type, has a slot located athwart to the electric field components for the lowest resonant mode, as shown in Fig. 10. Therefore, air discontinuity creates a noticeable perturbation of electromagnetic field and as a result it significantly shifts the resonant frequency. That is why the SDR shows much larger tunability than the binary DR. The resonant frequency of a basic mode variates up to tens percent while displacement of SDR parts is not more than tens or hundreds of micrometer depending on wavelength band and permittivity of dielectric material. This range of displacement can be achieved in modern piezo-actuators and MEMS.

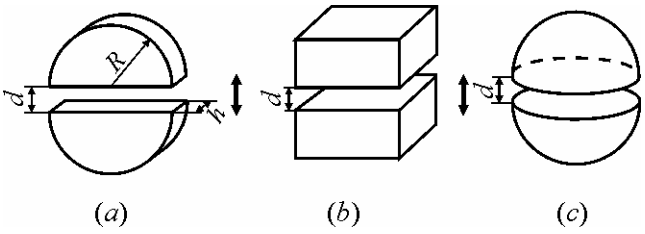

Fig. 10. Split dielectric resonators of various shapes: (*a*) disk, (*b*) rectangular, (*c*) spherical.

SDR tunability can be explained as alteration of its effective ε_{eff} permittivity, as depicted in Fig. 11*a*. In this case, the value of ε_{eff} decreases approximately by 2 times; SDR resonant frequency increases up to 30 percent or higher. Tunability slightly rises with the increase of the ratio *h*/*R* where *R* is the SDR radius, and *h* is its thickness.

An advantage of such frequency control method is preservation of high *Q*-factor. The unloaded quality factor can be expressed as follows:

$$Q_0^{-1} = T \tan\delta,$$

where *T* is the energy filling factor, dependent only on dielectric constant and domain size; $\tan\delta$ is the loss tangent of dielectric material. Fig. 11*b* shows that the *T*-factor trends to decrease with increasing of a slot width due to electromagnetic energy accumulation in a slot. As a result, the intrinsic *Q*-factor of the SDR can even rise with increasing of the resonant frequency.

The frequency control method can be applied to different shapes of SDR including rectangular (Fig. 10*b*), ring or sphere (Fig. 10*c*). Dependences of effective permittivity and energy filling factor versus a normalized air slot width for these shapes have a similar character as presented in Fig. 11 with some quantitative differences.

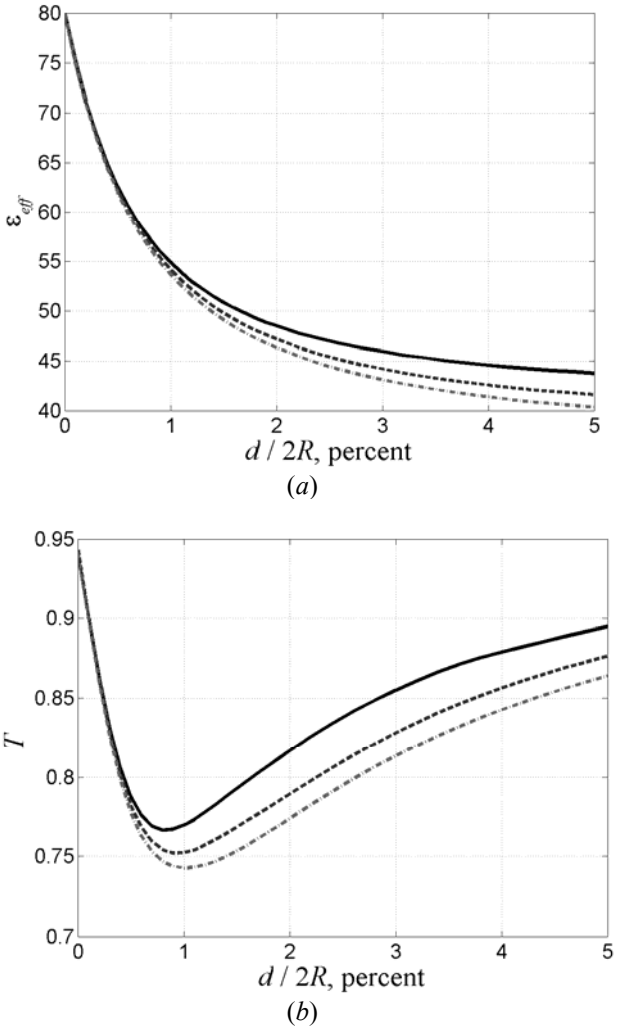

Fig. 11. Effective permittivity (*a*) and energy filling factor (*b*) versus a normalized value of air gap between two parts of disk DR shown in Fig. 10*b* for certain ratios of resonator thickness to its diameter: 0.3 (solid line); 0.5 (dashed line); 0.7 (dash-dot line). Permittivity of dielectric material is equal to 80; *R* is DR radius while *h* is DR thickness.

SDR controlled by the piezo-actuator or MEMS provides a model for high-quality tunable microwave filter in which central frequency as well as the shape of an attenuation frequency characteristic can be electrically controlled with rather a fast response. Based on these concepts, bandpass and bandstop frequency tuned

filters were realized [14, 15]. These filters are different from the known ones with their wide alteration bandwidth and high-quality Q-factor that remains stable while filter electromechanical control.

Electromechanically tunable microstrip phase shifter

Fig. 12 shows principal designs of the piezo-driven phase shifter based on the microstrip line. Experiments and calculations demonstrate that their phase shift is strongly dependent on the design architecture.

The design shown in Fig. 12*a* was previously presented [16]. However, it is obvious that other design shown in Fig. 12*b* is more effective because dielectric discontinuity is created in the plane perpendicular to the electrical field of the microstrip line. Their effectiveness was verified and proven experimentally. The best result is obtained for design with the detached upper electrode (Fig. 12*b*). This is the electrode disconnected with substrate and located onto the moveable dielectric plate. The phase shift akin to this case would be obtained if the bottom electrode was disconnected.

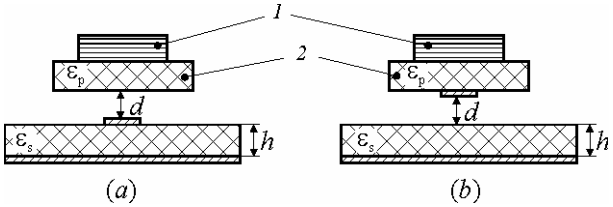

Fig. 12. Tunable microstrip lines with signal electrode on the substrate (*a*) and on the moving dielectric plate (*b*): (*1*) piezo-mover; (*2*) dielectric.

Propagation constant at a given frequency f can be estimated as

$$\gamma = \frac{2\pi f}{c}\sqrt{\varepsilon_{eff}} ,$$

where c is the light velocity. Alteration of effective permittivity ε_{eff} due to variation of air gap width d changes the propagation constant and provides a phase shift of the microstrip line section. So the main task of device analysis is to determine the effective permittivity for prescribed geometrical configuration. This problem was solved numerically using the finite element method [17].

Dependencies of effective permittivity of near 50 Ω microstrip lines shown in Fig. 12 as the functions of normalized air gap width is presented in Fig. 13. Permittivities of both substrate ε_s and dielectric plate ε_p are equal to 12. The microstrip line tunability with a detached upper electrode is higher than for the design presented in Fig. 12*a*. It should be noted that the microstrip line tunability with a disconnected bottom electrode remains between two designs considered but closer to the design with a detached upper electrode.

Fig. 13 shows that for the design with a detached upper electrode a significant alteration of effective permittivity can be achieved with the air gap variation of tens percents from substrate thickness. The displacement is available for piezo-actuators or MEMS.

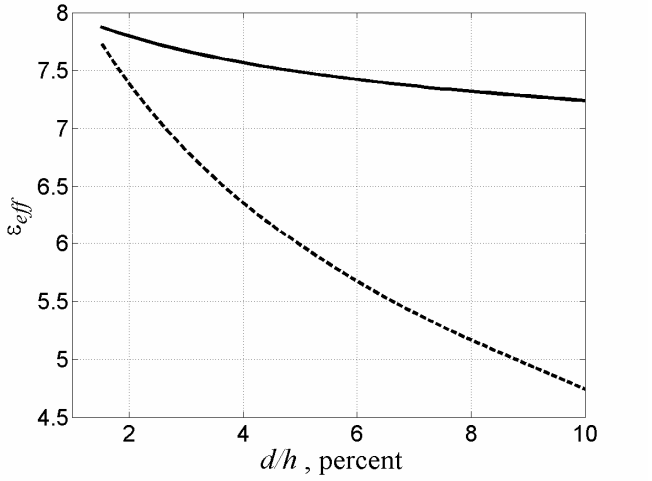

Fig. 13. Effective permittivity of microstrip lines presented in Fig. 12*a* (solid line) and Fig. 12*b* (dashed line) versus a normalized air gap. Characteristic impedance of the lines is near 50 Ω. Permittivities of both substrate and dielectric plate are equal to 12.

Electromechanically tunable coplanar line

Electromagnetic field of substrate deposited microwave transmission lines is mainly confined in the substrate right under electrodes as well as in the interelectrode space to a certain degree. The dielectric body travelling up and down above the line surface, as shown in Fig. 14*a*, makes a small perturbation of electromagnetic field distribution. To improve the device controllability it is necessary to arrange tighter dependence of electromagnetic field on moving dielectric body position. To this end, we propose to locate the signal strip of coplanar waveguide onto the moving dielectric body and let them lift together, as shown in Fig. 14*b*.

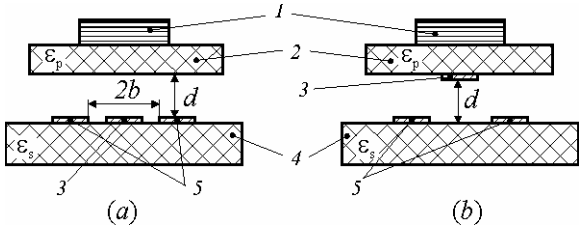

Fig. 14. Arrangements of phase shifters based on coplanar line with signal line on the fixed substrate (*a*) and on the moving dielectric body (*b*): *1* — piezo-mover; *2* — moving dielectric body; *3* — signal line; *4* — dielectric substrate; *5* — ground electrodes.

Fig. 15 shows the simulation results for near 50 Ω coplanar lines presented in Fig. 14 with dielectric permittivities of both substrate ε_s and movable dielectric body ε_p equal to 12. Quantitative data proves that the device with a detaching electrode exhibits a greater relative effective permittivity change under other similar conditions, and thus its relative phase shift more than 1.5 times exceeds the counterpart. Moreover, the control curve is less bended as well.

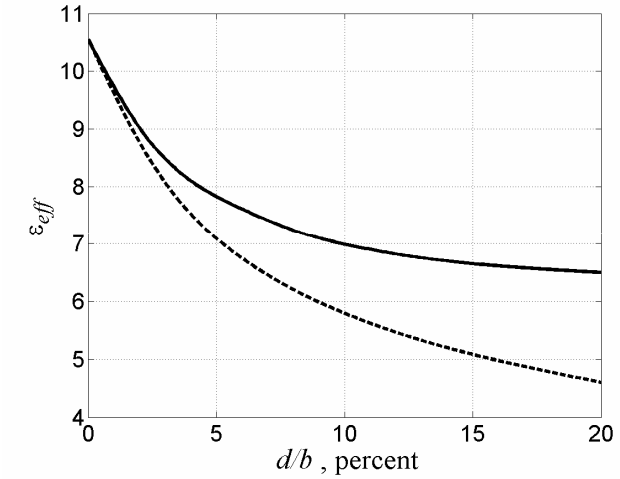

Fig. 15. Effective permittivity of coplanar lines presented in Fig. 14*a* (solid line) and Fig. 14*b* (dashed line) versus normalized air gap. Characteristic impedance of the lines is near 50 Ω. Permittivities of both substrate and dielectric body are equal to 12

Obviously, a strong perturbation of electromagnetic field improves the device controllability. But quantitatively it depends on a large number of design factors such as line geometry dimensions and the ratio of substrate and movable dielectric permittivities.

The analysis shows that the increase of movable dielectric permittivity leads to the increase of maximum possible relative phase shift for both designs, though its character is somewhat different. This effect can be explained by increasing the role of a high-permittivity body which confines a greater part of the line electromagnetic field, and thus leads to a larger rearrangement of the electromagnetic field in the device cross-section as a dielectric body moves away from the substrate.

The situation becomes quite different as the substrate permittivity varies. As the substrate permittivity increases, the influence of the moving body lowers. In contrast, with a detached electrode the effect of the electromagnetic field redistribution becomes stronger. The absolute values of the latter design exceed their counterparts at times.

The obtained results show that generally low lines impedance exhibits a higher controllability. This can be achieved not only by utilizing high-permittivity materials, but also by the proper layout as well.

To prove these ideas a scaled up experiment was performed. The experimental setup consisted of a coplanar dielectric ($\varepsilon = 4.3$) substrate in the aluminium fixture. The signal line is soldered to the bonding pad at the sides of the substrate (Fig. 16*a*), while being glued to the moveable dielectric, which in turn is attached to the micrometer screw (see Fig. 16*b*). This experimental setup was also used for investigation of microstrip line phase shifters. The phase measurement was performed as a two-port S-parameters measurement by Hewlett Packard 8753D network analyzer.

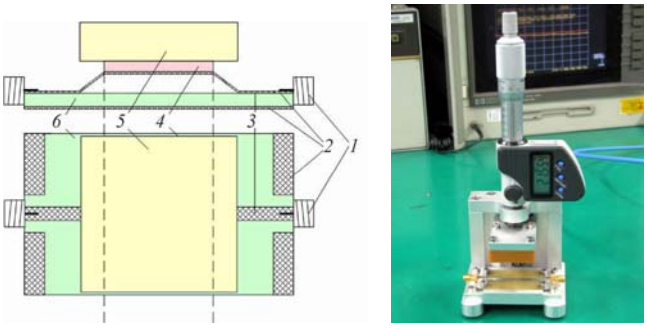

(*a*) (*b*)

Fig. 16. The experimental setup: (*a*) schematic (*1* — coaxial junction, *2* — ground electrodes, *3* — movable electrode, *4* — movable dielectric, *5* — low-permittivity support, *6* — substrate); (*b*) — photo.

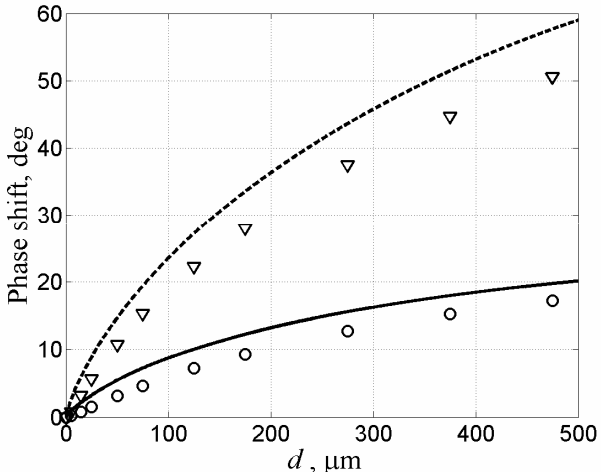

Fig. 17. Measured and simulated phase shift of the coplanar line controlled by teflon slab versus air gap at the frequency 5 GHz. For design presented in Fig. 14*a* simulated results are indicated by solid line while measured data are shown by circles. For design (Fig. 14*b*) simulated and measured data are depicted by dashed line and by triangles respectively. Substrate with permittivity $\varepsilon = 4.3$ have dimensions $40 \times 30 \times 1.6$ mm. Movable dielectric sizes are $30 \times 20 \times 1$ mm, its permittivity is equal to 2.08. Signal line width is 3 mm.

Fig. 17 presents the control curves of phase shift calculated from computer simulation and derived by measurements for both discussed designs at the frequency 5 GHz for the coplanar section length equal to 30 mm. A measured insertion loss was in the range from 0.5 dB at the frequency 1 GHz to 1.5 dB at the frequency 6 GHz. The simulation results agree well with the measured data as shown in Fig. 17.

Conclusions

Main mechanisms of piezoelectric or MEMS control of dielectric microwave devices were discussed. Particular attention was devoted to the investigation of the "microwave dielectric — air gap" composition controlled by the fast actuator. This composition ensures the minimal loss inserted in the tunable components.

To achieve electromechanical control by using piezo-actuators or MEMS the dielectric–air discontinuity should create significant perturbation of the electromagnetic field. It requires a certain location of the discontinuity relatively distribution of the electromagnetic field. For maximal reconfiguration of the electromagnetic field by displacement of dielectric parts, the border between the air and a dielectric should be perpendicular to the electrical filed component. In this case the displacement of dielectric parts leads to a considerable rearrangement of the electromagnetic field and as a result to alteration of device characteristics.

Using high-quality microwave dielectrics, it is possible to realize low loss filters and phase shifters in both microwaves and millimeter waves. Proposed structures were studied in the rectangular waveguide as well as in some microstrip and coplanar designs.

The proposed way of control allows increasing the device controllability while maintaining a low loss. Simulation results were verified and experimentally proved. While scaling down at a transfer to the higher frequencies, the amount of required displacements could be reduced to tens micrometers allowing utilization of small and fast piezo-actuators or MEMS.

References

1. Lucyszyn S. and Robertson I. D. Synthesis techniques for high performance octave bandwidth 180° analog phase shifters // IEEE Transactions on Microwave Theory and Techniques. — 1992. — Vol. 40, N. 4. — P. 731–740.

2. Lee C. S., Tran J. M. Coplanar waveguide semiconductor phase shifter // Microwave and Optical Technology Letters. — 1995. — Vol. 10, N. 2. — P. 100–102.

3. Ellinger F., Vogt R., Bachtold W. Compact reflective-type phase-shifter MMIC for C-band using a lumped-element coupler // IEEE Transactions on Microwave Theory and Techniques. — 2001. — Vol. 49, N. 5. — P. 913–917.

4. Rao J. B. L., Patel D. P., Krichevsky V. Voltage-controlled ferroelectric lens phased arrays // IEEE Transactions on Antennas and Propagation. — 1999. — Vol. 47, N. 3. — P. 458–468.

5. Deleniv A., Abadei S., Gevorgian S. Tunable ferroelectric filter-phase shifter // IEEE MTT-S International Microwave Symposium Digest. — June 2003. — Vol. 2. — P. 1267–1270.

6. Coplanar ferroelectric phase shifter on silicon substrate with TiO2 buffer layer / Ki-Byoung Kim, Tae-Soon Yun, Hyun-Suk Kim, et al. // Proceedings of European Microwave Conference EuMC-2005, Paris, October 4–6, 2005. — Vol. 1. — P. 649–652.

7. Demonstration of a photonically controlled RF phase shifter / S. S. Lee, A. H. Udupa, H. Erlig, et al. // IEEE Microwave Guided Wave Letters. — 1999. — N. 9. — P. 357–359.

8. Phase modulation efficiency and transmission loss of silicon optical phase shifters / Ling Liao, Ansheng Liu, R. Jones, et al. // IEEE Journal of Quantum Electronics. — 2005. — Vol. 41, N. 2. — P. 250–257.

9. Molchanov V. I., Yakimenko Yu. I., Pashkov V. M. Possibility of piezo-effect application for alteration of resonant frequency of solid state microwave filters // Proceedings of Conference "Problems in Microwave Integral Electronics", Leningrad, April 1984. — P.156 [in Russian].

10. Molchanov V. I., Pyatchanin S. V., Prokopenko Yu. V. Split dielectric resonator with air gap // Izvestiya Vuzov. Radioelectronics. — 1987. — N. 1. — P. 31–35 [in Russian].

11. Possibillities of electromechalical alteration of microwave oscillating systems / Yu. I. Yakimenko, S. A. Kravchuk, T. N. Naritnik, et al. // Izvestiya Vuzov. Radioelectronics. — 1988. — N. 10. — P. 50–56 [in Russian].

12. Yegorov Yu. V. Partially filled rectangular waveguides. — Moscow: Soviet Radio, 1967. — 214 p. [in Russian].

13. Ilchenko M. E., Kudinov E. V. Ferrite and dielectric microwave resonators. — Kiev: Kiev University publisher, 1973. — 175 p. [in Russian].

14. Frequency-tunable microwave dielectric resonator / Yu. M. Poplavko, Yu. V. Prokopenko, V. I. Molchanov, at al. // IEEE Transactions on Microwave Theory and Techniques. — 2001. — Vol. 49, N. 6. — P. 1020 — 1026.

15. Pratsiuk B. B., Prokopenko Yu. V., Poplavko Yu. M. Method of mistuning compensation for tunable filter based on dielectric resonators // Electronics and communications. — 2009. — Vol. 5, N. 2. — P. 19–22 [in Russian].

16. Yun T.-Y., Chang K. Analysis and optimization of a phase shifter controlled by a piezoelectric transducer // IEEE Transactions on Microwave Theory and Techniques. — 2002. — Vol. 50, N. 1. — P. 105–111.

17. Epitaxial BST thin film as microwave phase shifter / B. J. Kim, S. Baik, Y. Poplavko, Y. Prokopenko // Integrated Ferroelectrics. — 2001. — Vol. 34. — P. 207–214.

Received in final form July 19, 2010